Published OnlineFirst February 11, 2014; DOI: 10.1158/2326-6066.CIR-14-0019-T

Research Article

Cancer Immunology Research

Enhancing Efficacy of Anticancer Vaccines by Targeted Delivery to Tumor-Draining Lymph Nodes

Laura Jeanbart[1,2], Marie Ballester[1,2], Alexandre de Titta[1], Patricia Corthésy[1,2], Pedro Romero[4], Jeffrey A. Hubbell[1,3], and Melody A. Swartz[1,2,3]

Abstract

The sentinel or tumor-draining lymph node (tdLN) serves as a metastatic niche for many solid tumors and is altered via tumor-derived factors that support tumor progression and metastasis. tdLNs are often removed surgically, and therapeutic vaccines against tumor antigens are typically administered systemically or in non–tumor-associated sites. Although the tdLN is immune-suppressed, it is also antigen experienced through drainage of tumor-associated antigens (TAA), so we asked whether therapeutic vaccines targeting the tdLN would be more or less effective than those targeting the non-tdLN. Using LN-targeting nanoparticle (NP)-conjugate vaccines consisting of TAA-NP and CpG-NP, we compared delivery to the tdLN versus non-tdLN in two different cancer models, E.G7-OVA lymphoma (expressing the nonendogenous TAA ovalbumin) and B16-F10 melanoma. Surprisingly, despite the immune-suppressed state of the tdLN, tdLN-targeting vaccination induced substantially stronger cytotoxic $CD8^+$ T-cell responses, both locally and systemically, than non–tdLN-targeting vaccination, leading to enhanced tumor regression and host survival. This improved tumor regression correlated with a shift in the tumor-infiltrating leukocyte repertoire toward a less suppressive and more immunogenic balance. Nanoparticle coupling of adjuvant and antigen was required for effective tdLN targeting, as nanoparticle coupling dramatically increased the delivery of antigen and adjuvant to LN-resident antigen-presenting cells, thereby increasing therapeutic efficacy. This work highlights the tdLN as a target for cancer immunotherapy and shows how its antigen-experienced but immune-suppressed state can be reprogrammed with a targeted vaccine yielding antitumor immunity. *Cancer Immunol Res; 2(5); 436–47. ©2014 AACR.*

Introduction

As cancer remains a leading cause of death worldwide, active research is ongoing to develop new treatments that could replace or supplement classical cancer therapies, which include surgery, radiotherapy, and chemotherapy. Immunotherapies, which aim to activate the immune system to kill cancer cells, include strategies to increase the frequency or potency of antitumor T cells, to overcome suppressive factors in the tumor microenvironment, and to reduce T-cell suppression systemically (1–3). Despite promising results from clinical trials (4, 5), such immunotherapies can induce deleterious side effects in healthy nontargeted tissues (2, 3, 6). Furthermore, immunotherapy efficacy is often dampened by tumor-induced immune suppression, which occurs at the primary tumor site and extends to the tumor-draining lymph node (tdLN), thus allowing tumors to evade immune surveillance (6–8). Prophylactic vaccines exist against viruses that can drive certain types of cancer, such as human papillomavirus and hepatitis B virus (9). Therapeutic cancer vaccines, however, remain scarce because of the many challenges involved in breaking tolerance, permeating immunosuppressive barriers in the microenvironment, and attacking a heterogeneous tumor population with antigenic drift, just to name a few (2, 6, 7).

Targeting vaccines to dendritic cells (DC) with appropriate costimulation is crucial for the induction of antigen-specific cytotoxic $CD8^+$ T cells and Th1 cells, which are required to mount an effective antitumor response and to kill tumor cells (7, 10–13). Strategies based on delivering adjuvants or antigens carried by nanoparticles or liposomes have led to improved targeting of LNs, activation of LN-resident DCs, and enhanced induction of antigen-specific $CD8^+$ T cells, hence better protection in tumor challenge studies (14–19). Ultrasmall, functionalizable nanoparticles (NP) developed in our laboratory effectively target DCs in skin-draining LNs upon intradermal delivery (20, 21). These nanoparticles lead to antigen cross-presentation by DCs and to enhanced cytotoxic antigen-specific $CD8^+$ T-cell immunity when coupled with an antigen or an adjuvant (22–24).

LNs could be a strategic target for vaccine delivery because of their role in initiating adaptive immunity. Tumor-derived

Authors' Affiliations: [1]Institute of Bioengineering, School of Life Sciences and School of Engineering; [2]Swiss Institute for Experimental Cancer Research (ISREC), School of Life Sciences; [3]Institute for Chemical Sciences and Engineering, School of Basic Sciences, Ecole Polytechnique Fédérale de Lausanne (EPFL); and [4]Ludwig Center for Cancer Research, Université de Lausanne (UNIL), Lausanne, Switzerland

Note: Supplementary data for this article are available at Cancer Immunology Research Online (http://cancerimmunolres.aacrjournals.org/).

Corresponding Author: Melody A. Swartz, Institute of Bioengineering, School of Life Sciences and Engineering, EPFL, SV IBI LLCB, AI 1106, Lausanne, 1015, Switzerland. Phone: 41-21-693-9686; Fax: 41-21-693-9685; E-mail: melody.swartz@epfl.ch

doi: 10.1158/2326-6066.CIR-14-0019-T

Published OnlineFirst February 11, 2014; DOI: 10.1158/2326-6066.CIR-14-0019-T

factors and tumor-associated antigens (TAA), along with tumor-educated regulatory T cells (Treg) and myeloid-derived suppressor cells (MDSC), infiltrate the tdLN where they tolerize naïve T cells and prevent DC maturation, while minimally, or not at all, affecting non-tdLNs (8, 25, 26). In this fashion, the tdLN is an immune-privileged site that is remotely controlled and modified by the upstream tumor (25, 27). Although surgical removal of the tdLN along with the primary tumor is common practice in patients with breast cancer and melanoma (28, 29), targeting the tdLN with a cancer vaccine could take advantage of TAA-primed leukocytes in the tdLN and might enhance therapeutic efficacy and patient survival.

We asked whether specifically targeting the tdLN, which is already TAA primed but also drains immunosuppressive tumor-derived factors, with nanoparticle vaccines would be advantageous or disadvantageous for its efficacy as compared with targeting a naïve non-tdLN. To address this question, we conjugated either the model TAA ovalbumin (OVA) or the endogenous melanoma TAA tyrosinase-related protein-2 (TRP-2) and the TLR9 ligand CpG DNA to nanoparticles separately, and we therapeutically treated E.G7-OVA or B16-F10 tumor-bearing mice with this cancer vaccine. We first determined the therapeutic superiority of nanoparticle-conjugated TAA and CpG over their soluble form. Then, by therapeutic intradermal delivery of our nanoparticle vaccine, we found that targeting the tdLN, as opposed to the non-tdLN, elicited the strongest antitumor response in terms of tumor growth, survival, and effector $CD8^+$ T-cell response in both tumor models, and led to modulation of tumor-infiltrating immunosuppressive cells. Our findings demonstrate that although the tdLN is more immune suppressed than a non-tdLN, it is also TAA primed and can mount a more potent antitumor immune response than the non-tdLN. Thus, anticancer vaccines that target specifically the tdLN may be more effective, and at lower doses, than vaccines delivered at other sites.

Materials and Methods

Reagents

Chemicals were reagent grade and purchased from Sigma-Aldrich. CpG-B 1826 oligonucleotide (5′-TCCATGACGTTCCTGACGTT-3′), 5′ SPO_3-CpG, and 5′ SPO_3-CpG-NH_2 3′ were purchased from Microsynth. Low endotoxin grade OVA (<0.01 EU/μg protein) was from Hyglos; OVA grade V and $OVA_{257–264}$ peptide (SIINFEKL) were purchased from Sigma-Aldrich and GenScript, respectively. OVA, Alexa Fluor 488 conjugate, was purchased from Life Technologies. Endotoxins were removed with the EndoTrap red 10 kit from Hyglos and used according to the manufacturer's instructions. TRP-$2_{180–188}$ peptide (SVYDFFVWL) was purchased from AnaSpec, and C-TRP-$2_{180–188}$ (CSVYDFFVWL) was purchased from GenScript. DY633 NHS ester was purchased from Dyomics, and Alexa Fluor 647 C_2 maleimide was from Life Technologies.

Mice and cell lines

C57BL/6 female mice, ages 8 to 12 weeks, were obtained from Harlan. All experiments were performed with approval from the Veterinary Authority of the Canton de Vaud, Switzerland, according to Swiss law. E.G7-OVA (CRL-2113), EL-4 (TIB-39), and B16-F10 (CRL-6475) cells were obtained from the American Type Culture Collection and cultured according to the instructions. All cell lines were checked for *Mycoplasma*; no additional authentication was performed.

Tumor inoculation and immunizations

Mice were anesthetized with isoflurane (5% for induction and 2% for maintenance) and their backs were shaved. A total of 10^6 E.G7-OVA or EL-4 cells were injected in 30 μL of 0.9% saline solution intradermally on the left side of the back of each mouse. After 4, 7, or 11 days, mice were immunized with 10 μg of OVA and 1 μg of CpG (vaccine) in a dose of 30 μL intradermally in the front footpad ipsilaterally (ipsi) or contralaterally (contra) to the tumor. Mice received a boost 7 days after the immunization. Blood was sampled from the submandibular vein of the cheek pouch with a 4-mm lancet on the day of boost and then every 7 days thereafter.

For TRP-2 studies, 2.5×10^5 B16-F10 melanoma cells were injected intradermally on one side of the back such that lymphatic drainage from the tumor only flowed to the brachial LN (i.e., the tdLN) on one side. Mice were immunized on days 4, 7, 11, and 15 with either 40 μg TRP-2 and 4 μg CpG in all four footpads, or with 10 μg NP-TRP-2 plus 1 μg NP-CpG or 10 μg free CpG in the front footpad either ipsi or contra to the tumor. Blood was sampled on day 10.

Tumors were measured with a digital caliper starting 4 days after inoculation, and volumes (V) were calculated as ellipsoids ($V = \pi/6 \times$ length $\times$ width $\times$ height). Mice were sacrificed when tumor volumes reached 1 cm^3, as required by Swiss law.

Tissue and cell preparation

Spleens, brachial LNs, and tumors were harvested at the time of sacrifice. LNs and tumors were digested 30 and 90 minutes, respectively, in Dulbecco's Modified Eagle Medium (DMEM) supplemented with 1 mg/mL collagenase D (Roche). Single-cell suspensions were obtained by gently disrupting the organs through a 70-μm cell strainer. Red blood cells were lysed with NH_4Cl (ammonium chloride). Cells were counted and resuspended in Iscove's Modified Dulbecco's Medium (IMDM) supplemented with 10% FBS and 1% penicillin/streptomycin (full medium; all from Life Technologies). Serum was collected and stored at −20°C. Whole LN cell suspensions were plated in a black 96-well plate, and fluorescence was read on a plate reader.

For real-time PCR (RT-PCR), tumors were snap-frozen and homogenized in Lysing Matrix D tubes (MP Biomedicals). RNA was extracted with RNAqueous kit (Life Technologies) according to the manufacturer's instructions. OVA primers (forward, TCAACCAAATCACCAAACC; reverse, CCAAGCCTCCTCTATACAG) were purchased from Microsynth.

Ex vivo restimulation

A total of 2×10^6 spleen or 0.5×10^6 LN cells were plated in 96-well plates and cultured in full medium for 6 hours at 37°C in the presence of 1 μg/mL SIINFEKL peptide or 100 μg/mL OVA protein. Of note, 5 μg/mL brefeldin A (Sigma-Aldrich) was added to the culture for the last 3 hours of culture before analyzing cells by flow cytometry.

Published OnlineFirst February 11, 2014; DOI: 10.1158/2326-6066.CIR-14-0019-T

Other methods

Nanoparticle synthesis, conjugation, and labeling, flow cytometry, ELISA, and immunostaining are described in Supplementary Materials and Methods.

Statistical analysis

Statistically significant differences between experimental groups were determined by one-way ANOVA followed by Bonferroni posttest correction with Prism software (v5, GraphPad). Of note, * and ** indicate *P* values less than 0.05 and 0.01, respectively; n.s., not significant.

Results

The tdLN is enlarged and immune suppressed, but contains tumor antigen–primed T cells

Tumor-draining and nondraining brachial LNs were isolated from E.G7-OVA tumor-bearing mice at different time points of growth and analyzed by immunofluorescence and flow cytometry. Although we found that the tdLN was generally inflamed, as seen by size enlargement when compared with a non-tdLN (Fig. 1A), the overall distribution of different lymphocytes and the frequencies of $CD11b^+$ $MHCII^+$ macrophages (Mφ), $CD11c^+$ $MHCII^+$ DCs, and $CD11b^+$ $MHCII^-$ immature myeloid cells were not affected by the upstream tumor 11 days after tumor inoculation (Fig. 1B). Proportionally, there were more $B220^+$ B cells and fewer $CD3^+$ T cells present in the tdLN than in the non-tdLN (Fig. 1B). Overall, the tdLN contained fewer $CD8^+$ $CD11b^-$ cross-presenting DCs both as percentage of total live cells (Fig. 1C) and of all DCs (Fig. 1D) as compared with the non-tdLN. DCs in the tdLN expressed more PD-L1 than in the non-tdLN (Fig. 1E). Consistent with this observation, $CD8^+$ T cells expressed higher levels of PD-1 in the tdLN (Fig. 1F). As tumors progressed, more TAA-specific $CD8^+$ T cells infiltrated the tdLN, while the levels in the non-tdLN remained unchanged (Fig. 1G), as determined by SIINFEKL-MHCI pentamer staining. Upon *ex vivo* restimulation, $CD8^+$ T cells in the tdLN secreted more IFN-γ, TNF-α, and interleukin (IL)-2 than $CD8^+$ T cells isolated from the non-tdLN (Fig. 1H). Taken together, these results show that while being inflamed and immune suppressed, the tdLN is tumor antigen primed and responds to tumor antigen, whereas the non-tdLN is not immune suppressed and not tumor antigen primed.

Nanoparticles target the tdLN

Nanoparticles developed by our group target skin-draining LNs and resident antigen-presenting cells (APC) upon intradermal administration (20, 21). To determine whether nanoparticles could be targeted to the tdLN harnessing lymphatic drainage, we polarized one side of the mouse as being tumor-draining by inoculating 10^6 E.G7-OVA tumor cells intradermally on one side of the back of mice, thus defining an ipsi tumor-draining side and the contra non–tumor-draining side (Supplementary Fig. S1A). After intratumoral injection of 30 μL of propidium iodide (PI) solution 7 days after inoculation, PI accumulated in the ipsi brachial LN, thus identifying it as the tdLN in our model (Supplementary Fig. S1B, left).

To assess LN targeting by nanoparticles, we injected fluorescently labeled nanoparticles (NP^*, where * is Alexa Fluor 647; Supplementary Materials and Methods) intradermally in the front footpads on the ipsi or contra side 7 days after tumor inoculation. Nanoparticles injected on the contra side accumulated significantly more in the contra brachial LN, whereas ipsi-injected NP^* accumulated significantly more in the ipsi brachial LN (Supplementary Fig. S1B). Moreover, we found that contra-injected NP^* targeted DCs, defined as $CD11c^+$ $MHCII^+$, in both the contra and ipsi brachial LNs, whereas ipsi-injected NP^* targeted more the ipsi brachial and axillary LNs, being taken up by approximately 20% of the DCs resident in those LNs (Supplementary Fig. S1C). These data indicate that nanoparticles administered ipsi to the tumor accumulate in the tdLN and target resident DCs there, thereby providing an opportunity to modulate their behavior and potentially the tumor-associated immune responses.

Nanoparticle conjugation enhances cell targeting and therapeutic efficacy of OVA + CpG cancer vaccines

To explore the concept of antitumor vaccination targeted to the tdLN, we first engineered nanoparticle-conjugated antigen and adjuvant vaccines and explored their therapeutic efficacy in two different tumor models, namely the orthotopic and nonimmunogenic B16-F10 melanoma model and the E.G7-OVA model, a mouse lymphoma cell line (EL-4) that has been engineered to express OVA as model TAA.

We conjugated the TRP-$2_{180–188}$ peptide, an endogenous and thus centrally tolerized TAA, to nanoparticles by adding a cysteine at the N-terminus of TRP-$2_{180–188}$ (CSVYDFFVWL) to allow conjugation via a disulfide bond (Supplementary Materials and Methods). We used the TLR9-ligand CpG as adjuvant for its Th1-skewing properties (12) and ability to boost antitumor immunity (30–32). B16-F10–bearing mice were immunized intradermally in all four footpads 4, 7, 11, and 15 days after inoculation with 40 μg TRP-$2_{180–188}$ and 4 μg CpG conjugated onto nanoparticles (NP-TRP-2 + NP-CpG) or in soluble form (TRP-2 + CpG; Fig. 2A). The control group included nonimmunized mice. We found that nanoparticle-conjugated TRP-2 + CpG was therapeutically very efficient and superior to soluble TRP-2 + CpG, as seen by significantly smaller tumors and delayed tumor growth, as well as improved survival compared with mice immunized with soluble TRP-2 + CpG, which showed no improvement over control mice (Fig. 2B and C). Moreover, nanoparticle-immunized mice had approximately 5% circulating TRP-$2_{180–188}$–specific $CD8^+$ T cells 7 days after immunization, compared with 1% for mice immunized with TRP-2 and CpG in free form (Fig. 2D).

In the E.G7-OVA tumor model, conjugating the model antigen OVA to nanoparticles and codelivering it with NP-CpG was also therapeutically more beneficial than their soluble counterparts. E.G7-OVA tumor-bearing mice were ipsi immunized 4 days after inoculation and boosted 7 days later with 10 μg OVA and 1 μg CpG conjugated onto nanoparticles (NP-OVA + NP-CpG) or in soluble form (OVA + CpG; Fig. 2E). Control groups included nonimmunized tumor-bearing mice and NP-CpG–immunized mice (i.e., without antigen) to assess the contribution of innate immunity in the immune response to the vaccine. NP-OVA + NP-CpG significantly enhanced tumor regression compared with soluble OVA + CpG, as seen by

Published OnlineFirst February 11, 2014; DOI: 10.1158/2326-6066.CIR-14-0019-T

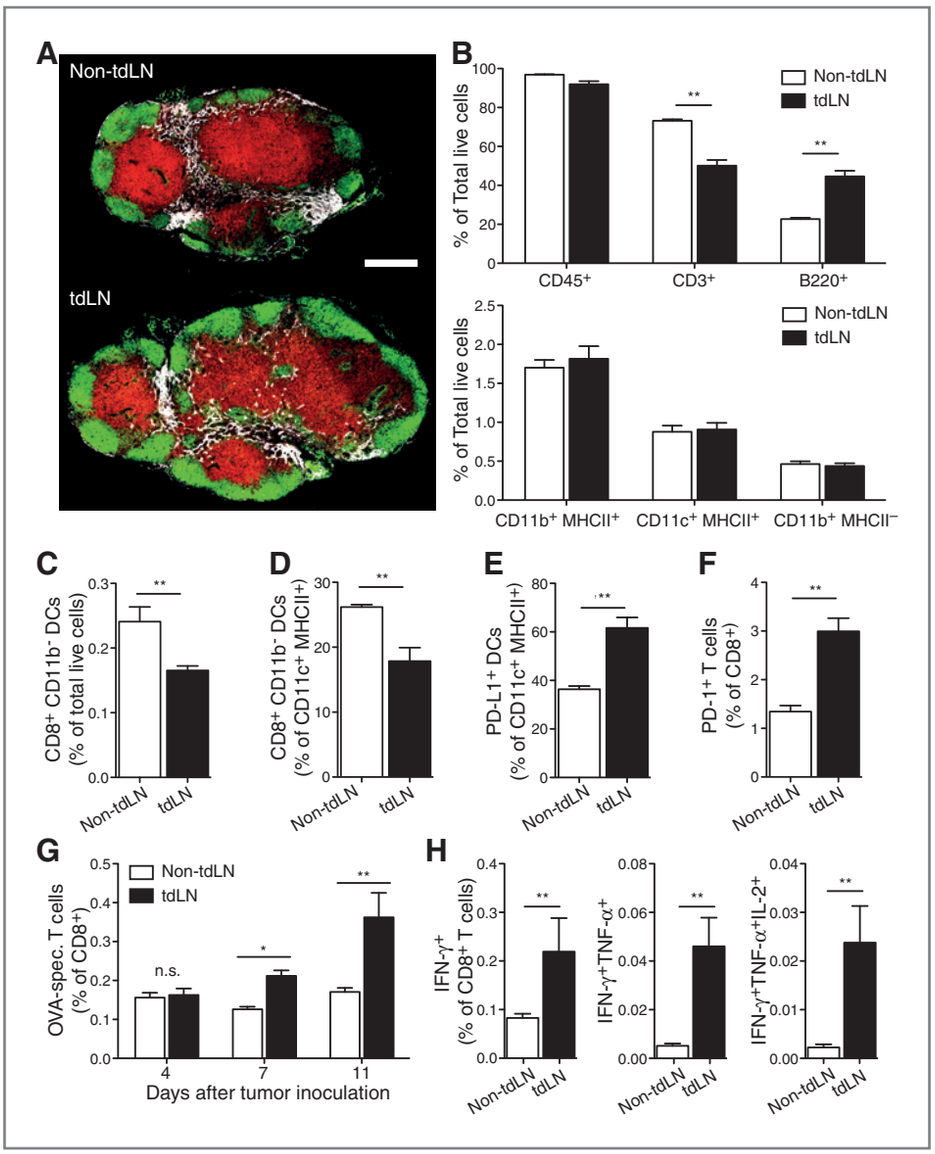

Figure 1. The tdLN is enlarged and immune suppressed, but contains tumor antigen–primed T cells. A total of 10^6 E.G7-OVA cells were inoculated intradermally on one side of the back such that tumor-draining and non–tumor-draining lymph nodes (tdLN and non-tdLN, respectively) could be compared at various time points. A, representative LN sections of tumor-bearing mice demonstrate enlargement of the tdLN compared with non-tdLN 14 days after tumor inoculation (white, lyve-1; red, CD3; green, B220); scale bar, 500 μm. B–H, characterization of LN-resident leukocytes 11 days after tumor inoculation. B, relative cell distributions show an increase in B- ($B220^+$) to T-cell ($CD3^+$) ratios in the tdLN versus non-tdLN, while percentages of total leukocytes ($CD45^+$) as well as macrophages ($CD11b^+$ $MHCII^+$), DCs ($CD11c^+$ $MHCII^+$), and immature myeloid cells ($CD11b^+$ $MHCII^-$) were unchanged 11 days after tumor inoculation. C and D, cross-presenting DCs ($CD8^+$ $CD11b^-$) as percentages of $CD11c^+$ $MHCII^+$ DCs (G) and total live cells (H). E, PD-L1 expression by mature DCs ($CD11c^+$ $MHCII^+$). F, PD-1 expression by $CD8^+$ T cells. G, relative numbers of LN-resident TAA-specific $CD8^+$ T cells as determined by SIINFEKL-MHCI pentamer staining on days 4, 7, and 11 after tumor inoculation. H, functionality of $CD8^+$ T cells after 6 hours restimulation as reflected by intracellular cytokine staining. Data reflect two independent experiments with 8 mice per group. *, $P < 0.05$; **, $P < 0.01$.

smaller tumor sizes and earlier onset of tumor regression (Fig. 2F and G). Moreover, NP-OVA + NP-CpG improved survival (Fig. 2H) and elicited 13% circulating $OVA_{257–264}$–specific $CD8^+$ T cells 7 days after immunization, whereas immunization with soluble OVA + CpG induced only 0.6% circulating $OVA_{257–264}$–specific $CD8^+$ T cells (Fig. 2I). NP-CpG, lacking antigen, did not affect therapeutic outcomes versus nonimmunized mice.

By fluorescent labeling of OVA (with Alexa Fluor 488) and of CpG (with Dy633; Supplementary Materials and Methods), we found that therapeutic efficacy of nanoparticle-conjugated antigen and adjuvant relied on enhanced APC targeting in the LNs. Because we had determined that the ipsi brachial LN was the tdLN in our tumor model (Supplementary Fig. S1B), we chose the symmetric contra brachial LN as non-tdLN. Nanoparticle-conjugated or soluble labeled OVA and labeled CpG were injected ipsi or contra to the tumor 7 days after inoculation, and mice were sacrificed 24 hours later. Noninjected tumor-bearing mice were used as control for gating purposes. Nanoparticle conjugation led to significantly more co-uptake of OVA and CpG together by Mφ, while it also significantly enhanced the uptake by DCs in the tdLN after ipsi injection (Fig. 2J). Similarly, delivering labeled NP-OVA + NP-CpG contra significantly enhanced the uptake of OVA and CpG by Mφ in the non-tdLN (Fig. 2K) compared with OVA + CpG. These results show a clear advantage of nanoparticle conjugation for OVA and CpG targeting to APCs in the tdLN.

The tdLN is a more effective vaccine target site than the non-tdLN for a tumor antigen, but a less effective site for a nontumor antigen

Although we found that the tdLN was tumor antigen primed but immune suppressed, we asked whether a tdLN or a non-tdLN would induce a stronger immune response to an

Published OnlineFirst February 11, 2014; DOI: 10.1158/2326-6066.CIR-14-0019-T

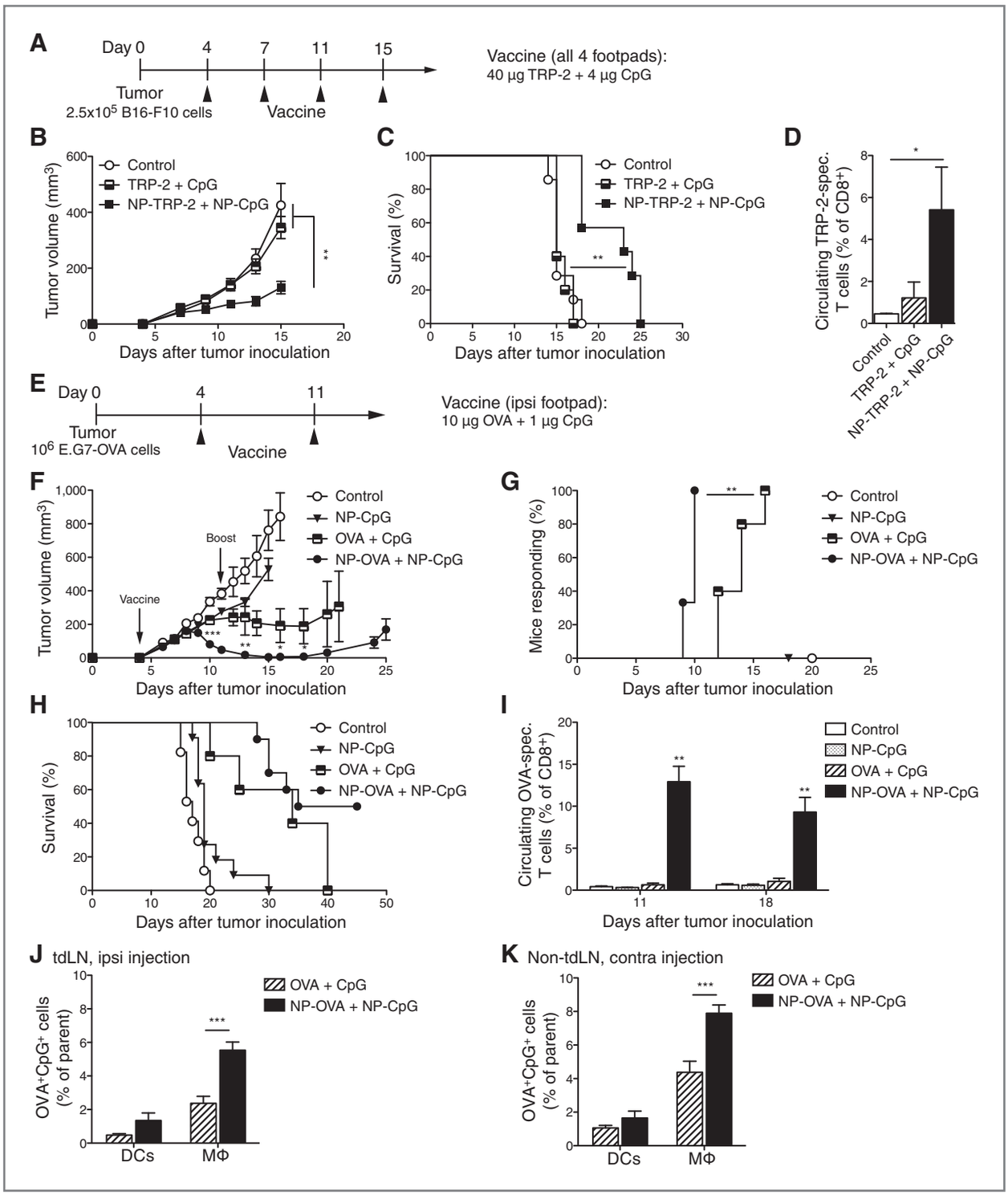

Figure 2. Nanoparticle conjugation enhances cell targeting and therapeutic efficacy of OVA + CpG cancer vaccines. Responses of B16-F10 (A–D) and E.G7-OVA (E–K) tumor-bearing mice to therapeutic vaccination are shown. Vaccination schedule (A), B16-F10 tumor volumes (B), overall survival rates (C), and circulating TRP-$2_{180–188}$–specific $CD8^+$ T cells (D) 11 days after tumor inoculation (as determined by TRP-$2_{180–188}$–MHCI pentamer staining). Vaccination schedule (E), E.G7-OVA tumor volumes (F), percentage of mice with tumor shrinkage after vaccination (G), overall survival rates (H), and circulating $OVA_{257–264}$–specific $CD8^+$ T cells (I) on days 11 and 18. J and K, on day 7 after tumor inoculation, E.G7-OVA tumor-bearing mice were injected intradermally with Alexa Fluor 488–labeled OVA and DY633-labeled CpG, either free or nanoparticle conjugated, in the front footpad either ipsi or contra to the tumor, and brachial LNs were analyzed 24 hours later. Nanoparticle conjugation leads to better targeting of OVA and CpG by mature macrophages (MΦ, $MHCII^+$ $CD11b^+$) and DCs ($MHCII^+$ $CD11c^+$) in the tdLN after ipsi injection (J) and in the non-tdLN after contra injection (K). Data reflect two independent experiments with 8 mice per group. *, $P < 0.05$; **, $P < 0.01$.

Published OnlineFirst February 11, 2014; DOI: 10.1158/2326-6066.CIR-14-0019-T

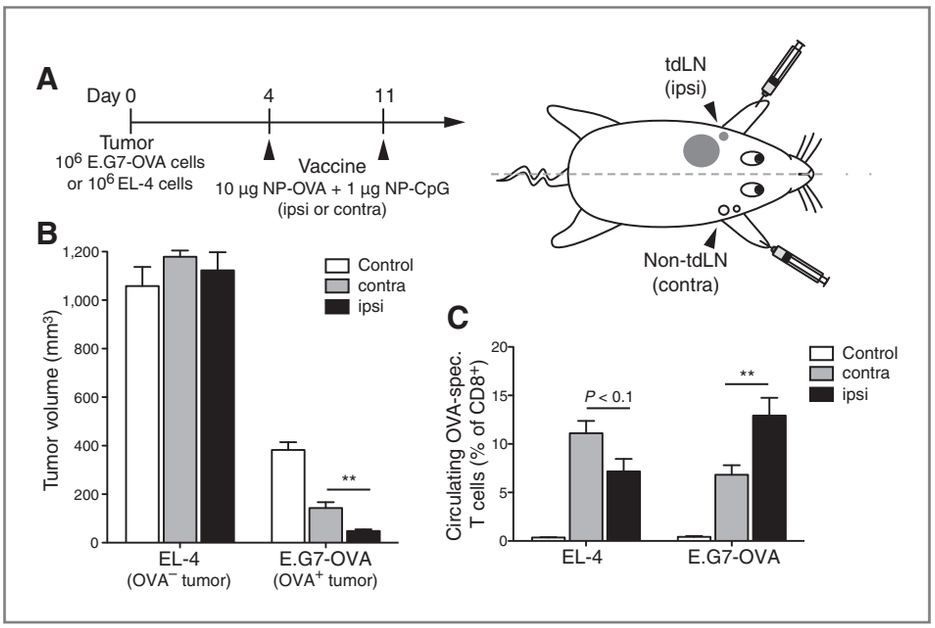

Figure 3. The tdLN is a more effective vaccine target site than the non-tdLN for a tumor antigen, but a less effective site for a nontumor antigen. Responses of EL-4 and E.G7-OVA tumor-bearing mice to therapeutic vaccination ipsi or contra to the tumor. A, vaccination schedule. B, day 11 tumor volumes, and C, circulating $OVA_{257–264}$–specific $CD8^+$ T cells 11 days after tumor inoculation in EL-4 versus E.G7-OVA tumor-bearing mice. Data reflect two independent experiments with 5 to 10 mice per group. **, $P < 0.01$.

irrelevant antigen. We immunized EL-4- and E.G7-OVA tumor-bearing mice with NP-OVA + NP-CpG ipsi or contra to the tumor and compared the immune response in both tumor models (Fig. 3A). Although E.G7-OVA tumors of immunized mice regressed as compared with control mice, EL-4 tumors were not affected by the vaccine 11 days after tumor inoculation (Fig. 3B). In the E.G7-OVA model, ipsi immunization with a TAA was more beneficial than contra immunization, as seen by tumor volumes and circulating $OVA_{257–264}$–specific $CD8^+$ T cells 11 days after tumor inoculation (Fig. 3B and C). However, contra immunization with NP-OVA + NP-CpG in the EL-4 tumor model led to more $OVA_{257–264}$–specific $CD8^+$ T cells in the blood than ipsi immunization (Fig. 3C). Taken together, these data indicate that targeting a tumor-irrelevant vaccine to a non-tdLN, which is not immune suppressed, is more beneficial than targeting a tdLN.

Therapeutic vaccines targeting the tdLN are more effective than those targeting the non-tdLN, but only after tumor growth has begun

After validation of nanoparticle-conjugated OVA and TRP-2 as effective therapeutic cancer vaccines, we used them as a tool to assess whether targeting the tdLN with a TAA is therapeutically different from targeting a non-tdLN. E.G7-OVA tumor-bearing mice were immunized ipsi or contra to the tumor with NP-OVA + NP-CpG at different stages of tumor growth, namely on day 4, 7, or 11 after inoculation. Blood was sampled 7, 14, and 21 days after immunization, and cells were stained with a SIINFEKL–MHCI-specific pentamer.

Both ipsi and contra day 4 vaccines induced regression of early-stage tumors. Ipsi immunization led to significantly smaller tumors on days 9 to 13 (Fig. 4A, top) and slightly enhanced survival (Fig. 4A, middle) compared with contra immunization. As seen by averaged results, ipsi delivery of day 4 vaccine induced significantly more circulating $OVA_{257–264}$–specific $CD8^+$ T cells than contra delivery 7 days after immunization (Fig. 4A, bottom). Targeting the tdLN of established tumors (day 7 ipsi) led to significantly smaller tumors on days 13 to 16 (Fig. 4B, top) compared with targeting the non-tdLN (day 7 contra). Of note, ipsi immunization on day 7 led to 100% survival (Fig. 4B, middle), as no tumors grew back after regressing, and to significantly more circulating $OVA_{257–264}$–specific $CD8^+$ T cells than contra delivery 7 days after immunization, with a 5-fold increase in $OVA_{257–264}$–specific $CD8^+$ T cells for ipsi vaccine compared with contra vaccine (Fig. 4B, bottom). At the latest immunization time point (day 11), ipsi injection of NP-OVA + NP-CpG afforded tumor regression of 1-cm^3 tumors, whereas contra delivery did not (Fig. 4C, top). Consequently, ipsi-immunized mice had significantly improved survival (Fig. 4C, middle). Although initially offering no advantage over contra vaccination in the blood, day 11 ipsi immunization led to approximately 15% antigen-specific $CD8^+$ T cells in the blood 14 days after immunization (Fig. 4C, bottom). NP-OVA + NP-CpG induced $OVA_{257–264}$–specific $CD8^+$ T cells with an activated, functional phenotype, i.e., $CD44^+$, $CD62L^-$, PD-$1^{+/-}$, CTLA-4^-, and LAG-3^- (Supplementary Fig. S2A). Finally, it is interesting to note that ipsi immunization with NP-OVA + NP-CpG also led to enhanced production of anti-OVA IgG antibodies 3 week after the day 4 vaccine compared with contra immunization (Supplementary Fig. S2B).

These findings were corroborated in the B16-F10 melanoma model with the peptide $TRP\text{-}2_{180–188}$ as TAA. Tumor-bearing mice were immunized with 10 μg NP-TRP-2 + 1 μg NP-CpG intradermally in the front footpad ipsi or contra to the tumor. Ipsi immunization resulted in significantly smaller tumors than those in control mice and led to improved survival compared with contra-immunized mice (Fig. 4D and E). Furthermore, ipsi immunization led to over 5% circulating $TRP\text{-}2_{180–188}$–specific $CD8^+$ T cells 7 days after immunization, as opposed to 2.5% in contra-immunized mice (Fig. 4F). Even when comparing with immunization of melanoma-bearing mice with a higher dose of free CpG (10 μg, a dose that we cannot easily achieve with nanoparticle-conjugated CpG)

Published OnlineFirst February 11, 2014; DOI: 10.1158/2326-6066.CIR-14-0019-T

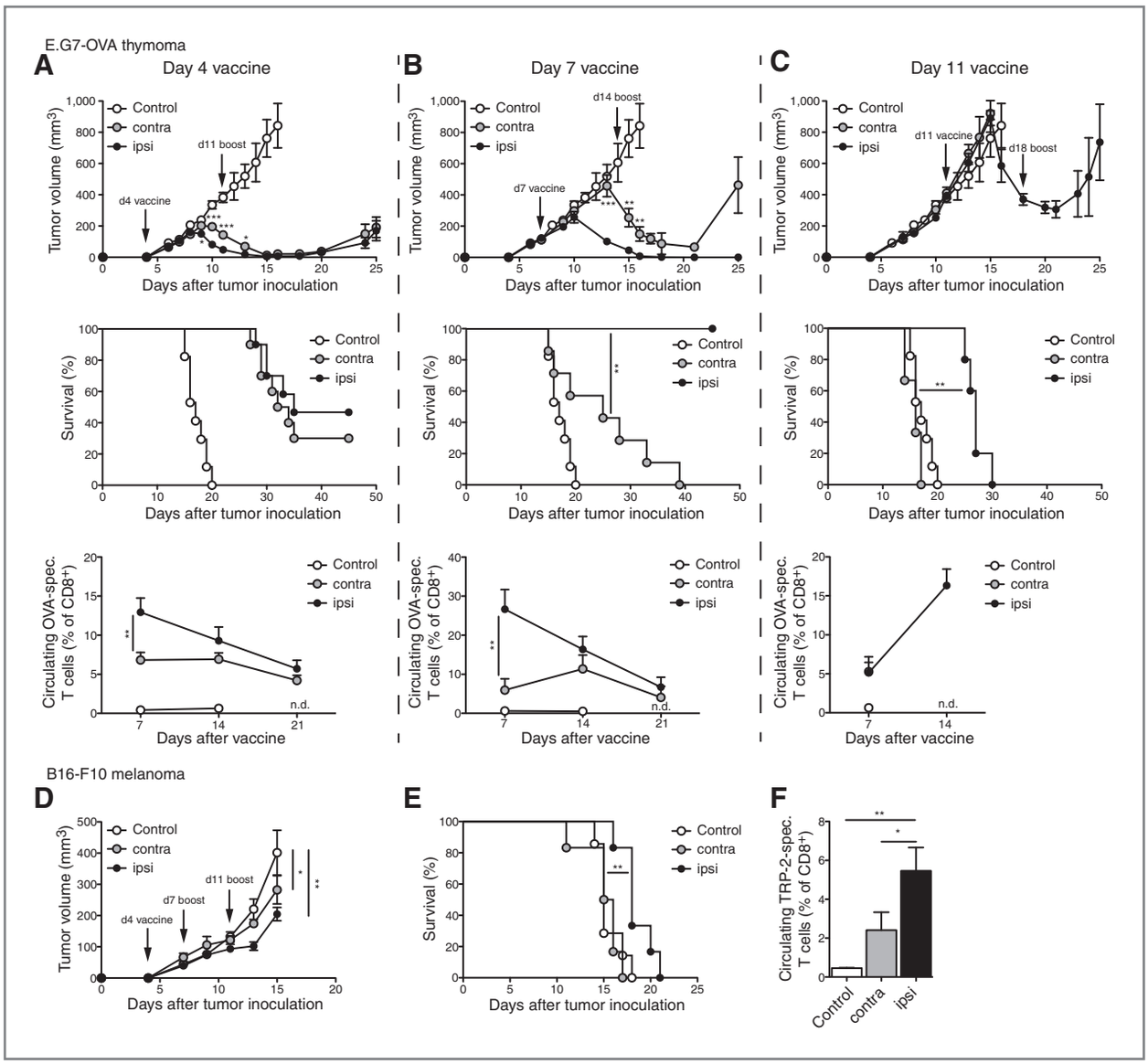

Figure 4. Therapeutic vaccines targeting the tdLN are more effective than those targeting the non-tdLN, but only after tumor growth has begun. Response of E.G7-OVA tumor-bearing mice to therapeutic vaccination with 10 μg NP-OVA + 1 μg NP-CpG ipsi or contra to the tumor 4 days (A), 7 days (B), or 11 days (C) after tumor inoculation: tumor volumes (top), survival (middle), and proportions of circulating $OVA_{257–264}$–specific $CD8^+$ T cells (bottom) 7, 14, and 21 days after vaccination of immunized and control mice (n.d., no data; statistics, ipsi vs. contra). A, at 4 days after inoculation, before tumors are visible, there is very little difference between vaccinating the tdLN versus the non-tdLN in terms of tumor response. B, in contrast, when vaccinated after 7 days, when tumors are visible and have presumably affected the tdLN, large differences are seen between contra versus ipsi vaccination, and only the ipsi-vaccinated group survives with no tumor regrowth. C, when mice are vaccinated at day 11 of tumor growth, which is close to the size limit before death or sacrifice is necessary, only the tdLN-targeted group can be rescued, while the non–tdLN-targeted group show no response to the vaccine. Response of B16-F10 melanoma-bearing mice after vaccination with 10 μg NP-TRP-$2_{180–188}$ + 1 μg NP-CpG ipsi or contra to the tumor: tumor volumes (D), survival (E), and proportions (F) of circulating TRP-$2_{180–188}$–specific $CD8^+$ T cells 11 days after tumor inoculation of immunized and control B16-F10 tumor-bearing mice. Data reflect several independent experiments with 5 to 10 mice per group. *, $P < 0.05$; **, $P < 0.01$; n.s., not significant $P > 0.05$.

along with NP-TRP-2 (10 μg as usual), the benefit of targeting the tdLN compared with the non-tdLN with a NP-TAA vaccine is evident (Supplementary Fig. S3A and S3B). The observed tumor regression and humoral responses, consistent both in the E.G7-OVA and B16-F10 models, highlight the advantage of delivering cancer vaccines to the tdLN for improved therapeutic antigen-specific tumor outcomes.

Targeting a nanoparticle vaccine to the tdLN enhances the effector $CD8^+$ T-cell response locally and systemically

With a cancer vaccine, induction of an antigen-specific effector immune response locally in the tdLN and especially in the tumor is key to obtaining tumor regression. To address this question and to understand the mechanisms behind the previous findings, we sacrificed mice at the peak of the vaccine-

Published OnlineFirst February 11, 2014; DOI: 10.1158/2326-6066.CIR-14-0019-T

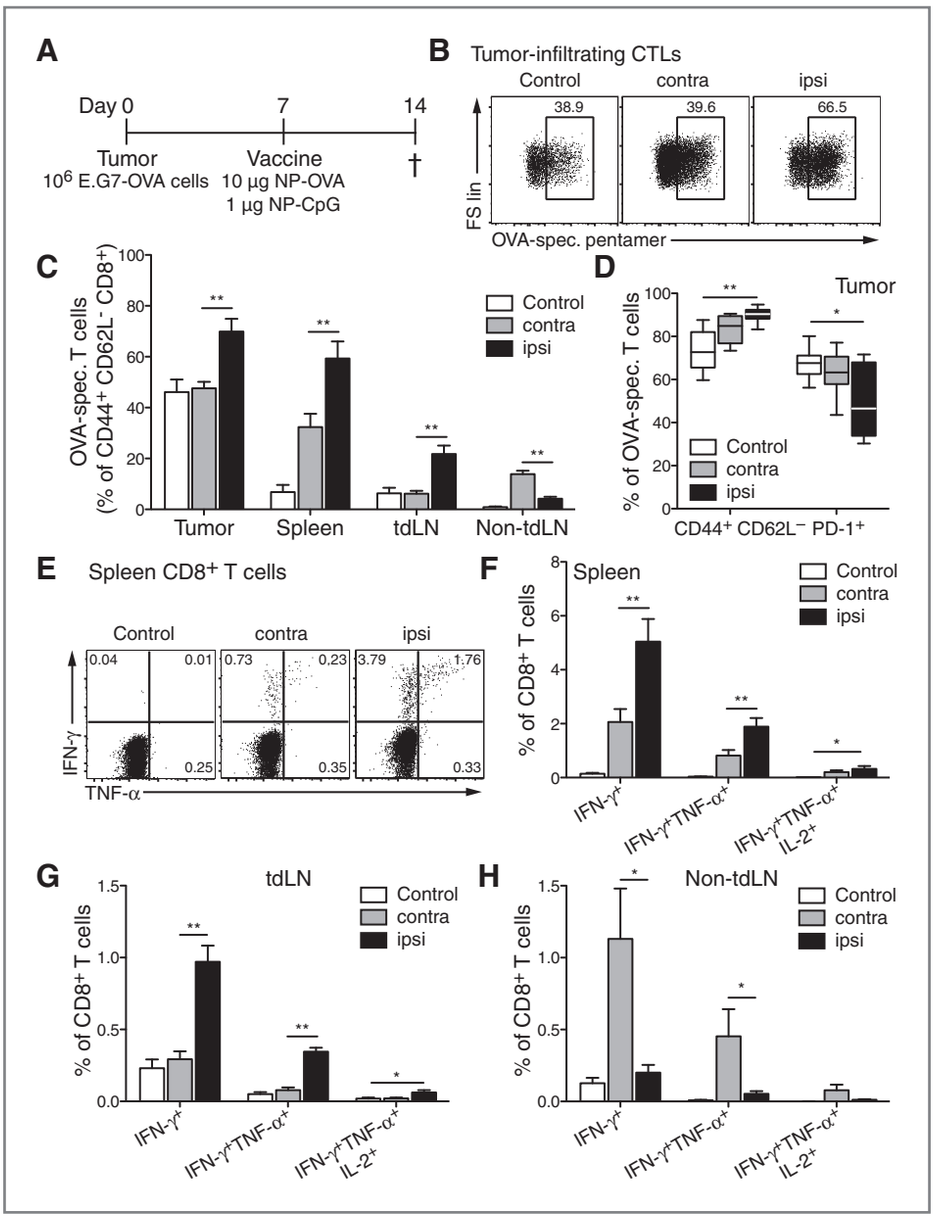

Figure 5. Targeting a nanoparticle vaccine to the tdLN enhances the effector $CD8^+$ T-cell response locally and systemically. $CD8^+$ T-cell responses 7 days after vaccination in E.G7-OVA tumor-bearing mice immunized with 10 μg NP-OVA + 1 μg NP-CpG ipsi or contra to the tumor. A, vaccination schedule. B, representative flow cytometry plots of SIINFEKL–MHCI pentamer staining of tumor-infiltrating CTLs ($CD44^+$ $CD62L^-$ effector $CD8^+$ T cells). C, proportion of $OVA_{257–264}$–specific CTLs ($CD44^+$ $CD62L^-$ effector $CD8^+$ T cells) in the tumor, spleen, tdLN, and non-tdLN as determined by SIINFEKL–MHCI pentamer staining. D, tumor-infiltrating $OVA_{257–264}$–specific $CD8^+$ T cells with an effector ($CD44^+$ $CD62L^-$) versus an exhausted ($PD\text{-}1^+$) phenotype. E–H, cells from spleens and LNs were restimulated *ex vivo* with SIINFEKL (1 μg/mL) for 6 hours before staining for intracellular cytokines and analysis by flow cytometry. E, representative flow cytometry plots of spleen $CD8^+$ T cells stained for IFN-γ^+ and TNF-α^+. Values in the dot plots represent the percentage of $CD8^+$ T cells in each gate. Proportion of IFN-γ^+, IFN-γ^+ TNF-α^+, and IFN-γ^+ TNF-α^+ IL-2^+ cytotoxic $CD8^+$ T cells in the spleen (F), tdLN (G), and non-tdLN (H) of ipsi, contra, and control mice after SIINFEKL restimulation. Data reflect two independent experiments with 8 mice per group. *, $P < 0.05$; **, $P < 0.01$.

induced T-cell response. Briefly, E.G7-OVA tumor-bearing mice were immunized with NP-OVA + NP-CpG 7 days after tumor inoculation ipsi or contra to the tumor and sacrificed 7 days later (Fig. 5A), which corresponded to the time point of peak number of circulating $OVA_{257–264}$–specific $CD8^+$ T cells and tumor regression (Fig. 4). Ipsi immunization led to enhanced infiltration of $CD8^+$ T cells (Supplementary Fig. S4A) and $OVA_{257–264}$–specific $CD8^+$ T cells (Supplementary Fig. S4B) in the tumor. As seen by representative flow cytometry plots (Fig. 5B), ipsi NP-OVA + NP-CpG enhanced tumor-infiltrating $OVA_{257–264}$–specific effector $CD8^+$ T cells (defined as $CD44^+$ $CD62L^-$), with almost 70% of effector $CD8^+$ T cells in the tumor being antigen-specific, compared with 40% for contra and control mice. Targeting the tdLN (ipsi) also induced significantly more $OVA_{257–264}$–specific effector $CD8^+$ T cells in the spleen and tdLN compared with contra immunization (Fig. 5C), which induced significantly more $OVA_{257–264}$–specific effector $CD8^+$ T cells in the non-tdLN than ipsi immunization (Fig. 5C). Similar results were obtained when all $CD8^+$ T cells and effector $CD8^+$ T cells were considered in the tumor, spleen, and tdLN (Supplementary Fig. S4B). Of note, tumor-infiltrating $CD8^+$ and $OVA_{257–264}$–specific $CD8^+$ T cells expressed more effector markers ($CD44^+$ $CD62L^-$) and less PD-1 in ipsi-immunized mice than in contra-immunized and control mice (Supplementary Fig. S4C and Fig. 5D).

In a cancer vaccine, it is important that T cells be licensed to kill tumor cells and thus secrete cytotoxic factors when encountering cells expressing tumor antigens (7, 33). Cells from the spleens, tdLN, and non-tdLN were restimulated *ex vivo* with the full OVA protein or its immunodominant peptide

Published OnlineFirst February 11, 2014; DOI: 10.1158/2326-6066.CIR-14-0019-T

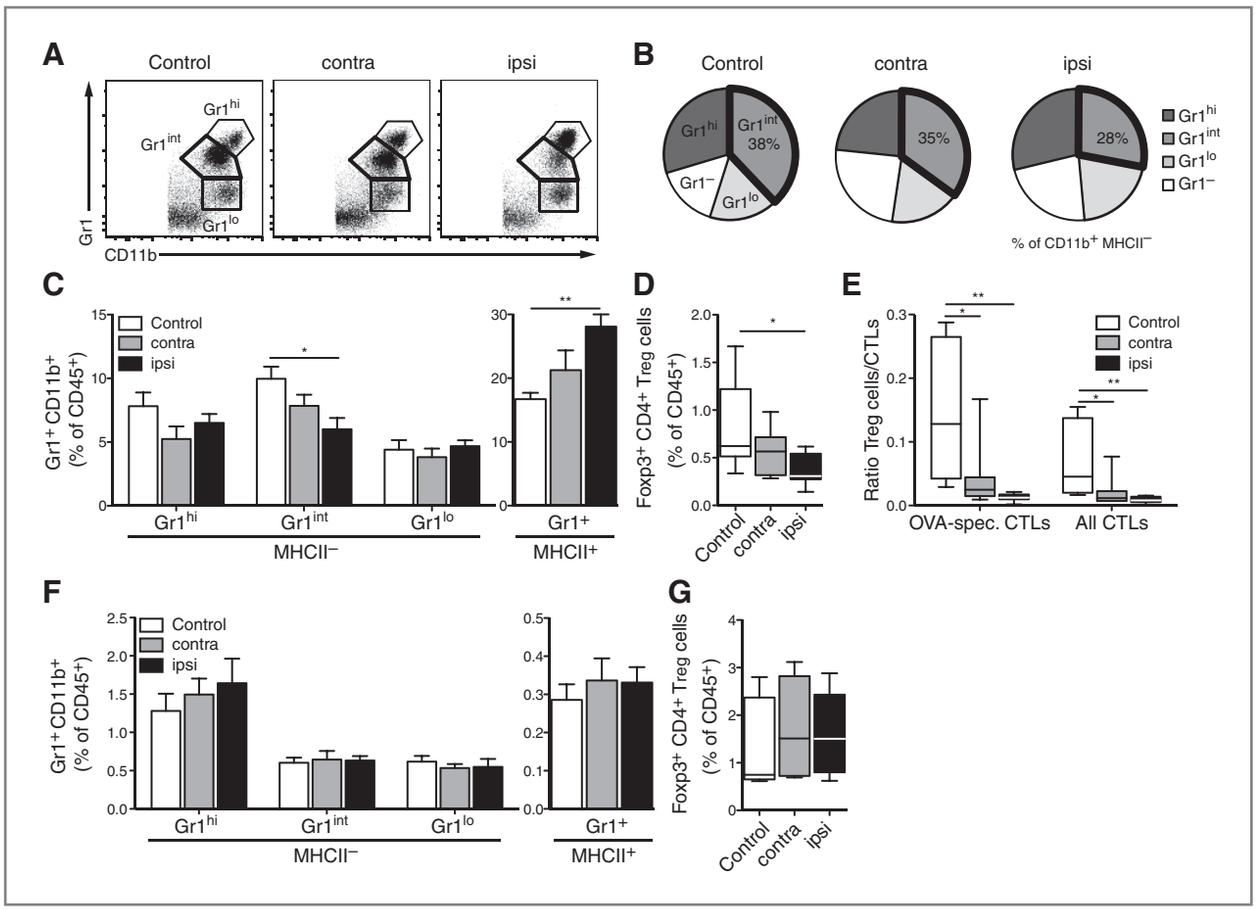

Figure 6. Targeting the tdLN with nanoparticle-conjugated OVA and CpG reduces the frequencies of tumor-infiltrating MDSCs and Tregs. Mice were immunized as described in Fig. 5A. Tumors (A–E) and spleens (F–G) were collected and analyzed by flow cytometry. A and B, representative flow cytometry plots (A) and pie charts (B) of Gr1-stained $CD11b^+$ $MHCII^-$ immature myeloid cells in the tumor: cells were gated on $CD11b^+$ $MHCII^-$ cells and numbers indicate the proportion of $Gr1^{hi}$, $Gr1^{int}$, and $Gr1^{lo}$ cells as a percentage of $CD11b^+$ $MHCII^-$. C, frequencies of $Gr1^+$ $CD11b^+$ cells as a percentage of $CD45^+$ cells: immature $MHCII^-$ cells (left) and mature $MHCII^+$ cells (right). D, frequency of $Foxp3^+$ $CD4^+$ Tregs as a percentage of $CD45^+$ cells. E, ratio of $Foxp3^+$ $CD4^+$ Tregs to all CTLs ($CD44^+$ $CD62L^-$ effector $CD8^+$ T cells) and to $OVA_{257–264}$–specific CTLs in the tumor. F and G, frequencies of immature ($MHCII^-$, left) and mature ($MHCII^+$, right) $Gr1^+$ $CD11b^+$ cells (F) and frequency of $Foxp3^+$ $CD4^+$ Tregs (G) as a percentage of $CD45^+$ cells in the spleen. Data reflect two independent experiments with 8 mice per group. *, $P < 0.05$; **, $P < 0.01$.

SIINFEKL for 6 hours and then stained for intracellular cytokines. As shown by representative flow cytometry plots and averaged results, targeting the tdLN with NP-OVA + NP-CpG (ipsi) led to 5% IFN-γ^+, 2% IFN-γ^+ TNF-α^+, and 1% triple-positive IFN-γ^+ TNF-α^+ IL-2^+ cytotoxic $CD8^+$ T cells in the spleen upon SIINFEKL restimulation, which are significantly more when compared with vaccines targeting the non-tdLN (contra; Fig. 5E and F). Similarly, ipsi immunization induced significantly more polyfunctional $CD4^+$ T cells than contra immunization as indicated by OVA restimulation on cells from the spleens (Supplementary Fig. S5A and S5B). Delivering NP-OVA + NP-CpG to the tdLN (ipsi) induced significantly more IFN-γ- and TNF-α–secreting cytotoxic $CD8^+$ T cells (Fig. 5G) and polyfunctional $CD4^+$ T cells (Supplementary Fig. S5C) in the tdLN compared with targeting the non-tdLN and control mice. Contra administration of NP-OVA + NP-CpG also led to a cytotoxic $CD8^+$ (Fig. 5H) and polyfunctional $CD4^+$ (Supplementary Fig. S5D) T-cell response in the non-tdLN, while ipsi delivery had no effect. These results illustrate the role of the tdLN in the induction of a potent effector T-cell response both systemically and locally in the tdLN and tumor, which is where tumor antigen recognition and tumor cell killing happen, respectively.

Targeting the tdLN with nanoparticle-conjugated OVA and CpG reduces the frequencies of tumor-infiltrating MDSCs and Tregs

Immunosuppressive cells, such as MDSCs and $Foxp3^+$ $CD4^+$ Tregs, contribute to tumor-induced tolerance (34, 35) and classically hinder cancer immunotherapies, making them an important target when designing cancer vaccines (7). Here, the goal was to assess whether targeting a nanoparticle-based vaccine to a tdLN could have an impact on the aforementioned cells locally in the tumor. To investigate this, we analyzed tumor-infiltrating cells from NP-OVA + NP-CpG–immunized mice (experiment setup as in Fig. 5A). Targeting the tdLN (ipsi)

Published OnlineFirst February 11, 2014; DOI: 10.1158/2326-6066.CIR-14-0019-T

led to a decrease in the proportion of tumor-infiltrating $Gr1^{int}$-expressing MDSCs (defined as $Gr1^+$ $CD11b^+$ $MHCII^-$), as shown by representative flow cytometry plots and averaged results (Fig. 6A and B). $Gr1^{int}$ MDSCs represented 28% of tumor-infiltrating $CD11b^+$ $MHCII^-$ cells in ipsi-immunized mice, compared with 35% and 38% in contra-immunized and control mice, respectively. Moreover, not only was the proportion of $Gr1^{int}$ cells among MDSCs reduced by ipsi immunization with NP-OVA + NP-CpG, the total number of $Gr1^{int}$ MDSCs also decreased in the tumor (Fig. 6C), while leaving the $Gr1^{hi}$, $Gr1^{lo}$, and $Gr1^-$ cells unaffected compared with contra-immunized and control mice. Interestingly, $Gr1^{int}$ MDSCs were recently shown to be the most immunosuppressive MDSCs in tumor-bearing mice (36). Furthermore, we observed that significantly more $MHCII^+$-expressing $CD11b^+$ $Gr1^+$ MDSCs infiltrated the tumors of tdLN-targeted (ipsi) mice compared with control and non–tdLN-targeted (contra) mice, suggesting maturation of MDSCs (Fig. 6C, left). Indeed, one promising approach to inhibit the immunosuppressive ability of MDSCs has been the induction of their maturation into APCs (37). Targeting the tdLN (ipsi) also led to a decrease in tumor-infiltrating $Foxp3^+$ $CD4^+$ Tregs (Fig. 6D), and to a more immunogenic, less suppressive Tregs to effector T-cell ratio (Fig. 6E). The proportions of MDSCs and Tregs decreased locally in the tumor microenvironment but were left unaffected by the nanoparticle vaccine systemically as seen in the spleen (Fig. 6F and G). Taken together, these data suggest that targeting the tdLN with a therapeutic cancer vaccine can also affect the tumor microenvironment locally by decreasing the number of immunosuppressive cells, both MDSCs and Tregs.

Discussion

In this study, we explored the use of a therapeutic nanoparticulate cancer vaccine platform to target the antigen-experienced, yet immune-suppressed tdLN of tumor-bearing mice. We found that this strategy was substantially more beneficial in terms of inducing a potent adaptive cellular immune response, both enhancing the numbers of antigen-specific CTLs and reducing the numbers of suppressive MDSCs and Tregs in the tumor, which correlated with reduction in tumor volume and prolongation of survival. Results from this study indicate that antigen-experience outweighs immune suppression in the tdLN, an immune organ whose role in clinical oncology should be reconsidered as it may play a useful role in facilitating cancer vaccination.

The tdLN is usually regarded as a site with prevailing immune suppression and tolerance to the upstream tumor (25, 27). We found that with tumor progression, the tdLN contained more $OVA_{257–264}$–specific $CD8^+$ T cells and that tdLN-resident $CD8^+$ T cells were more responsive to antigen stimulus than those in a non-tdLN as seen by cytokine secretion, but that the tdLN was also enlarged and immune suppressed as seen by enhanced PD-1 and PD-L1 expression by T cells and DCs, respectively (Fig. 1; ref. 2). We hypothesized that targeting a nanoparticle-based vaccine to the tdLN could break immune suppression and boost already TAA-primed immune cells in the tdLN.

Upon intradermal injection, sufficiently small nanoparticles take advantage of interstitial flow into the dermal lymphatics to efficiently drain through lymphatic vessels and target skin-draining LNs (21). Although intratumor, intra-LN, or subcutaneous administrations have been explored to target LNs with cancer immunotherapies, our experimental model permitted passive but direct and efficient targeting of nanoparticles from the skin to the tdLN (Supplementary Fig. S1; refs. 17, 31, 38). Our nanoparticles were in the range of 30 nm, thus smaller than particles used in many vaccination studies, hence affording enhanced lymphatic drainage and targeting of the skin-draining LNs (14–19).

To address our hypothesis, we first engineered nanoparticle cancer vaccines by conjugating the endogenous peptide $TRP\text{-}2_{180–188}$ and the nonendogenous model antigen OVA to the surface of nanoparticles and codelivered them with NP-CpG. Nanoparticle conjugation led to the induction of more antigen-specific $CD8^+$ T cells and stronger therapeutic outcomes, benefits that relied on enhanced dual targeting of APCs in the LNs (Fig. 2). Compared with current published studies, our TRP-2–based therapeutic nanoparticle vaccine is very potent at the low doses used for antigen and adjuvant (18, 39, 40). Similarly, other studies have shown improved therapeutic outcomes by either conjugating the adjuvant or the antigen onto or into delivery systems, such as poly(lactide-co-glycolide) particles and liposomes, but, to our knowledge, this is the first study to show enhanced co-uptake of both adjuvant and antigen by LN-resident APCs after nanoparticle conjugation (14–19). Furthermore, it has been shown recently that encapsulating antigens or TLR agonists in nanoparticles enhanced humoral responses compared with immunization with soluble antigen or adjuvant (41, 42).

By comparing delivery of our model cancer vaccine with the tdLN versus a non-tdLN, we found that targeting the tdLN afforded significantly improved tumor reduction and survival both in the E.G7-OVA and the aggressive B16-F10 melanoma mouse models (Fig. 4 and Supplementary Fig. S3). This was associated with a stronger antigen-specific effector immune response, in terms of cytotoxic $CD8^+$ T cells and polyfunctional $CD4^+$ Th1 cells, both systemically and locally in the tumor and the tdLN (Fig. 5 and Supplementary Fig. S5). Furthermore, efficient LN targeting by nanoparticles and conjugation of CpG onto nanoparticles allowed a very low dose of CpG (1 μg/mouse) to be effective, while typically much higher doses of free CpG (8–100 μg) are needed for effective adjuvant function (14–16, 18). Our results showed that the vaccine-induced local immune response in the tdLN translated to greater tumor reduction than the one elicited in a non-tdLN. This complements our previous study using adjuvant targeting alone; specifically, we demonstrated that NP-CpG or NP-paclitaxel targeted to the tdLN could partially reverse the immune-suppressed milieu there to slow tumor growth (43). In that study, however, the therapeutic benefit of adjuvant alone was very moderate compared with the present study with TAA-targeting vaccines (e.g., as shown in Fig. 4).

The very high number of circulating $OVA_{257–264}$–specific $CD8^+$ T cells (up to 30%; Fig. 4B) induced by targeting the vaccine to the tdLN led to regression of early-stage tumors and

Published OnlineFirst February 11, 2014; DOI: 10.1158/2326-6066.CIR-14-0019-T

more impressively of tumors having reached the Swiss legal limit of 1 cm^3. In the literature, cancer vaccines are usually administered when the tumors are 5 to 7 mm in diameter or even before they are detectable, and also do not usually induce this high number of TAA-specific $CD8^+$ T cells in the blood and the LNs (17, 19, 30, 38, 44), thus emphasizing the benefits of nanoparticle-mediated targeting of antigen and adjuvant to DCs in the tdLN (18, 38, 45). We noted, however, that after regressing some tumors grew back. OVA-transfected tumor cells can lose OVA expression over time (46, 47), a trend that we also observed by RT-PCR analysis of OVA expression at days 4, 7, and 11 after tumor inoculation (Supplementary Fig. S6); the loss of TAA expression may explain why some tumors grew back after regressing.

Finally, targeting the tdLN with nanoparticle-conjugated OVA and CpG affected the tumor microenvironment by reducing the frequency of immunosuppressive cells, including MDSCs and Tregs, while leaving those cells unaffected systemically (Fig. 6). While we previously showed that tumor-infiltrating monocytic MDSCs are NP^+, delivering our model cancer vaccine to the tdLN decreased the number of tumor-resident $Gr1^{int}$ MDSCs, which are described as monocytic and the most immunosuppressive subset, and led to MDSC maturation, thus making them less suppressive (21, 36, 48). CpG has been shown to affect the phenotype of MDSCs, especially monocytic MDSCs, in tumor-bearing mice, but at much higher CpG doses than we used here (32, 49). We believe that our findings may be due to an effect of CpG on MDSCs and to a change in the cellular and cytokine environment in the tumor following immunization. We noted a decrease in the frequency of Tregs and a subsequent reduction in the ratio of Tregs to effector $CD8^+$ T cells, suggestive of a benefit in antitumor response (50, 51). These findings indicate that the model cancer vaccine is shifting the balance from a tolerogenic to an immunogenic microenvironment in the tumor. Similarly, other studies have found that Tregs infiltrated the tdLN less when targeted with a cellular therapy in tumor-bearing mice (44).

Here, we show that the tdLN may be capable of playing a special role for the induction of a strong TAA-specific immune response using TAA vaccines, its antigen experience outweighing its immune suppressed state. Our results also show the advantage of using nanocarriers that are sufficiently small to drain to the LNs and to deliver adjuvants and antigens to resident APCs for effective induction of immune responses; this drainage enabled tdLN targeting. Finally, on the basis of our results in tumor models with both exogenous and endogenous antigens, we believe that delivering cancer immunotherapies to the tdLN is more effective than targeting them to a non-tdLN. In conclusion, this study shows the important role played by the tdLN in the induction of a potent antigen-specific immune response to a nanoparticle-based cancer vaccine; our results show that the benefits of TAA experience in the tdLN outweigh the detriments of exposure to immunosuppressive cytokines produced by the tumor.

Disclosure of Potential Conflicts of Interest

J.A. Hubbell and M.A. Swartz have ownership interest (including patents) in Lanta Bio Sàrl. No potential conflicts of interest were disclosed by the other authors.

Authors' Contributions

Conception and design: L. Jeanbart, P. Romero, J.A. Hubbell, M.A. Swartz
Development of methodology: L. Jeanbart, M. Ballester, A. de Titta, M.A. Swartz
Acquisition of data (provided animals, acquired and managed patients, provided facilities, etc.): L. Jeanbart, M.A. Swartz
Analysis and interpretation of data (e.g., statistical analysis, biostatistics, computational analysis): L. Jeanbart, M.A. Swartz
Writing, review, and/or revision of the manuscript: L. Jeanbart, J.A. Hubbell, M.A. Swartz
Administrative, technical, or material support (i.e., reporting or organizing data, constructing databases): P. Corthésy
Study supervision: M.A. Swartz

Acknowledgments

The authors thank A.W. Lund, M. Fankhauser, M. Rincon-Restrepo, A.J. van der Vlies, I.C. Kourtis, and the Flow Cytometry Core Facility of the EPFL for technical help and insightful discussion.

Grant Support

This study was supported by Fondation Recherche Suisse contre le Cancer (OncoSuisse, KFS-02696-08-2010), Carigest SA, the Swiss National Science Foundation (31-13576), and the European Research Council (NanoImmune).

The costs of publication of this article were defrayed in part by the payment of page charges. This article must therefore be hereby marked *advertisement* in accordance with 18 U.S.C. Section 1734 solely to indicate this fact.

Received January 31, 2014; accepted February 4, 2014; published OnlineFirst February 11, 2014.

References

1. Gajewski TF. Cancer immunotherapy. Mol Oncol 2012;6:242–50.
2. Mellman I, Coukos G, Dranoff G. Cancer immunotherapy comes of age. Nature 2011;480:480–9.
3. Sharma P, Wagner K, Wolchok JD, Allison JP. Novel cancer immunotherapy agents with survival benefit: recent successes and next steps. Nat Rev Cancer 2011;11:1–8.
4. Brahmer JR, Tykodi SS, Chow LQM, Hwu W-J, Topalian SL, Hwu P, et al. Safety and activity of anti–PD-L1 antibody in patients with advanced cancer. N Engl J Med 2012;366:2455–65.
5. Topalian SL, Hodi FS, Brahmer JR, Gettinger SN, Smith DC, McDermott DF, et al. Safety, activity, and immune correlates of anti–PD-1 antibody in cancer. N Engl J Med 2012;366:2443–54.
6. Motz GT, Coukos G. Deciphering and reversing tumor immune suppression. Immunity 2013;39:61–73.
7. Vanneman M, Dranoff G. Combining immunotherapy and targeted therapies in cancer treatment. Nat Rev Cancer 2012;12:1–15.
8. Cochran AJ, Huang R-R, Lee J, Itakura E, Leong SPL, Essner R. Tumour-induced immune modulation of sentinel lymph nodes. Nat Rev Immunol 2006;6:659–70.
9. Swartz MA, Hirosue S, Hubbell JA. Engineering approaches to immunotherapy. Sci Transl Med 2012;4:148rv9.
10. Palucka K, Banchereau J. Cancer immunotherapy via dendritic cells. Nat Rev Cancer 2012;12:265–77.
11. Banchereau J, Steinman RM. Dendritic cells and the control of immunity. Nature 1998;392:245–52.
12. Chu RS, Targoni OS, Krieg AM, Lehmann PV, Harding CV. CpG oligodeoxynucleotides act as adjuvants that switch on T helper 1 (Th1) immunity. J Exp Med 1997;186:1623–31.
13. Akira S, Takeda K. Toll-like receptor signalling. Nat Rev Immunol 2004;4:499–511.
14. Standley SM, Mende I, Goh SL, Kwon YJ, Beaudette TT, Engleman EG, et al. Incorporation of CpG oligonucleotide ligand into protein-loaded

Published OnlineFirst February 11, 2014; DOI: 10.1158/2326-6066.CIR-14-0019-T

particle vaccines promotes antigen-specific CD8 T-cell immunity. Bioconjug Chem 2007;18:77–83.
15. Bourquin C, Anz D, Zwiorek K, Lanz A-L, Fuchs S, Weigel S, et al. Targeting CpG oligonucleotides to the lymph node by nanoparticles elicits efficient antitumoral immunity. J Immunol 2008;181:2990–8.
16. Jong S, Chikh G, Sekirov L, Raney S, Semple S, Klimuk S, et al. Encapsulation in liposomal nanoparticles enhances the immunostimulatory, adjuvant and anti-tumor activity of subcutaneously administered CpG ODN. Cancer Immunol Immunother 2007;56:1251–64.
17. Jewell CM, López SCB, Irvine DJ. *In situ* engineering of the lymph node microenvironment via intranodal injection of adjuvant-releasing polymer particles. Proc Natl Acad Sci U S A 2011;108:15745–50.
18. Jérôme V, Graser A, Müller R, Kontermann RE, Konur A. Cytotoxic T lymphocytes responding to low dose TRP2 antigen are induced against B16 melanoma by liposome-encapsulated TRP2 peptide and CpG DNA adjuvant. J Immunother 2006;29:294–305.
19. Zhang Z, Tongchusak S, Mizukami Y, Kang YJ, Ioji T, Touma M, et al. Induction of anti-tumor cytotoxic T cell responses through PLGA-nanoparticle mediated antigen delivery. Biomaterials 2011;32:3666–78.
20. van der Vlies AJ, O'Neil CP, Hasegawa U, Hammond N, Hubbell JA. Synthesis of pyridyl disulfide-functionalized nanoparticles for conjugating thiol-containing small molecules, peptides, and proteins. Bioconjug Chem 2010;21:653–62.
21. Kourtis IC, Hirosue S, de Titta A, Kontos S, Stegmann T, Hubbell JA, et al. Peripherally administered nanoparticles target monocytic myeloid cells, secondary lymphoid organs and tumors in mice. PLoS ONE 2013;8:e61646.
22. Hirosue S, Kourtis IC, van der Vlies AJ, Hubbell JA, Swartz MA. Antigen delivery to dendritic cells by poly(propylene sulfide) nanoparticles with disulfide conjugated peptides: cross-presentation and T cell activation. Vaccine 2010;28:7897–906.
23. Nembrini C, Stano A, Dane KY, Ballester M, van der Vlies AJ, Marsland BJ, et al. Nanoparticle conjugation of antigen enhances cytotoxic T-cell responses in pulmonary vaccination. Proc Natl Acad Sci U S A 2011;108:E989–97.
24. de Titta A, Ballester M, Julier Z, Nembrini C, Jeanbart L, van der Vlies AJ, et al. Nanoparticle conjugation of CpG enhances adjuvancy for cellular immunity and memory recall at low dose. Proc Natl Acad Sci U S A 2013;110:19902–7.
25. Munn DH, Mellor AL. The tumor-draining lymph node as an immune-privileged site. Immunol Rev 2006;213:146–58.
26. McDonnell AM, Robinson BWS, Currie AJ. Tumor antigen cross-presentation and the dendritic cell: where it all begins? Clin Dev Immunol 2010;2010:1–9.
27. de Visser KE, Eichten A, Coussens LM. Paradoxical roles of the immune system during cancer development. Nat Rev Cancer 2006;6:24–37.
28. Takeuchi H, Kitajima M, Kitagawa Y. Sentinel lymph node as a target of molecular diagnosis of lymphatic micrometastasis and local immunoresponse to malignant cells. Cancer Sci 2008;99:441–50.
29. Alitalo K. The lymphatic vasculature in disease. Nat Med 2011;17:1371–80.
30. Miconnet I, Koenig S, Speiser D, Krieg A, Guillaume P, Cerottini J-C, et al. CpG are efficient adjuvants for specific CTL induction against tumor antigen-derived peptide. J Immunol 2002;168:1212–8.
31. Nierkens S, den Brok MH, Garcia Z, Togher S, Wagenaars J, Wassink M, et al. Immune adjuvant efficacy of CpG oligonucleotide in cancer treatment is founded specifically upon TLR9 function in plasmacytoid dendritic cells. Cancer Res 2011;71:6428–37.
32. Shirota Y, Shirota H, Klinman DM. Intratumoral injection of CpG oligonucleotides induces the differentiation and reduces the immunosuppressive activity of myeloid-derived suppressor cells. J Immunol 2012;188:1592–9.
33. Wilde S, Sommermeyer D, Leisegang M, Frankenberger B, Mosetter B, Uckert W, et al. Human antitumor $CD8^+$ T cells producing Th1 polycytokines show superior antigen sensitivity and tumor recognition. J Immunol 2012;189:598–605.
34. Zitvogel L, Tesniere A, Kroemer G. Cancer despite immunosurveillance: immunoselection and immunosubversion. Nat Rev Immunol 2006;6:715–27.
35. Park HJ, Kusnadi A, Lee E-J, Kim WW, Cho BC, Lee IJ, et al. Tumor-infiltrating regulatory T cells delineated by upregulation of PD-1 and inhibitory receptors. Cell Immunol 2012;278:76–83.
36. Ugel S, Peranzoni E, Desantis G, Chioda M, Walter S, Weinschenk T, et al. Immune tolerance to tumor antigens occurs in a specialized environment of the spleen. Cell Reports 2012;2:1–12.
37. Gabrilovich D, Nagaraj S. Myeloid-derived suppressor cells as regulators of the immune system. Nat Rev Immunol 2009;9:162–74.
38. Smith KA, Meisenburg BL, Tam VL, Pagarigan RR, Wong R, Joea DK, et al. Lymph node-targeted immunotherapy mediates potent immunity resulting in regression of isolated or metastatic human papillomavirus-transformed tumors. Clin Cancer Res 2009;15:6167–76.
39. Castle JC, Kreiter S, Diekmann J, Lower M, van de Roemer N, de Graaf J, et al. Exploiting the mutanome for tumor vaccination. Cancer Res 2012;72:1081–91.
40. Ly LV, Sluijter M, van der Burg SH, Jager MJ, van Hall T. Effective cooperation of monoclonal antibody and peptide vaccine for the treatment of mouse melanoma. J Immunol 2012;190:489–96.
41. Kasturi SP, Skountzou I, Albrecht RA, Koutsonanos D, Hua T, Nakaya HI, et al. Programming the magnitude and persistence of antibody responses with innate immunity. Nature 2011;470:543–7.
42. Moon JJ, Suh H, Li AV, Ockenhouse CF, Yadava A, Irvine DJ. Enhancing humoral responses to a malaria antigen with nanoparticle vaccines that expand T_{fh} cells and promote germinal center induction. Proc Natl Acad Sci U S A 2012;109:1080–5.
43. Thomas SN, Vokali E, Lund AW, Hubbell JA, Swartz MA. Targeting the tumor-draining lymph node with adjuvanted nanoparticles reshapes the anti-tumor immune response. Biomaterials 2014;35:814–24.
44. Zhang Y, Wakita D, Chamoto K, Narita Y, Matsubara N, Kitamura H, et al. Th1 cell adjuvant therapy combined with tumor vaccination: a novel strategy for promoting CTL responses while avoiding the accumulation of Tregs. Int Immunol 2006;19:151–61.
45. Zaks K, Jordan M, Guth A, Sellins K, Kedl R, Izzo A, et al. Efficient immunization and cross-priming by vaccine adjuvants containing TLR3 or TLR9 agonists complexed to cationic liposomes. J Immunol 2006;176:7335–45.
46. Breckpot K, Dullaers M, Bonehill A, Van Meirvenne S, Heirman C, De Greef C, et al. Lentivirally transduced dendritic cells as a tool for cancer immunotherapy. J Gene Med 2003;5:654–67.
47. Beaudette TT, Bachelder EM, Cohen JA, Obermeyer AC, Broaders KE, Fréchet JMJ, et al. *In vivo* studies on the effect of co-encapsulation of CpG DNA and antigen in acid-degradable microparticle vaccines. Mol Pharm 2009;6:1160–9.
48. Gabrilovich DI, Ostrand-Rosenberg S, Bronte V. Coordinated regulation of myeloid cells by tumours. Nat Rev Immunol 2012;12:253–68.
49. Zoglmeier C, Bauer H, Norenberg D, Wedekind G, Bittner P, Sandholzer N, et al. CpG blocks immunosuppression by myeloid-derived suppressor cells in tumor-bearing mice. Clin Cancer Res 2011;17:1765–75.
50. Bui JD. Comparative analysis of regulatory and effector T cells in progressively growing versus rejecting tumors of similar origins. Cancer Res 2006;66:7301–9.
51. Sato E, Olson SH, Ahn J, Bundy B, Nishikawa H, Qian F, et al. Intraepithelial $CD8^+$ tumor-infiltrating lymphocytes and a high $CD8^+$/regulatory T cell ratio are associated with favorable prognosis in ovarian cancer. Proc Natl Acad Sci U S A 2005;102:18538–43.

Published OnlineFirst February 11, 2014; DOI: 10.1158/2326-6066.CIR-14-0019-T

Cancer Immunology Research

Enhancing Efficacy of Anticancer Vaccines by Targeted Delivery to Tumor-Draining Lymph Nodes

Laura Jeanbart, Marie Ballester, Alexandre de Titta, et al.

Cancer Immunol Res 2014;2:436-447. Published OnlineFirst February 11, 2014.